Available online at www.sciencedirect.com
ScienceDirect
Trans. Nonferrous Met. Soc. China 21(2011) 2476−2483
Transactions of Nonferrous Metals Society of China
www.tnmsc.cn

Numerical simulation of acoustic pressure field for ultrasonic grain refinement of AZ80 magnesium alloy

SHAO Zhi-wen, LE Qi-chi, ZHANG Zhi-qiang, CUI Jian-zhong

Key Laboratory of Electromagnetic Processing of Materials of Ministry of Education, Northeastern University, Shenyang 110004, China

Received 21 October 2010; accepted 15 March 2011

Abstract: Ultrasound with different intensities was applied to treating AZ80 alloy melt to improve its solidification structure. The average grain size of the alloy could be decreased from 303 to 148 μm after the ultrasound with intensity of 30.48 W/cm^2 was applied. To gain insight into the mechanism of ultrasonic treatment which affected the microstructure of the alloy, numerical simulations were carried out and the effects of different ultrasonic pressures on the behaviors of cavitation bubble in the melt were studied. The ultrasonic field propagation in the melt was also characterized. The results show that samples from different positions are subjected to different acoustic pressures and the effect of grain refinement by ultrasonic treatment for these samples is different. With the increase of ultrasonic intensity, the acoustic pressure is increased and the grain size is decreased generally.

Key words: numerical simulation; acoustic pressure; ultrasonic treatment; grain refinement; magnesium alloy

1 Introduction

Owing to its comprehensive advantages, including low density, high specific strength and stiffness, excellent machinability, superior damping and magnetic shielding capacities, magnesium alloy has a great prospect of applications in various fields, such as aviation and spaceflight, automobile and computer manufacturing, communication and optic instruments [1−3]. However, it also has its own inherent defects, such as low strength and poor toughness, which limit the application of magnesium alloy to a large extent. Therefore, it is of great importance to improve the strength and toughness of magnesium alloy. Due to the fact that mechanical properties are dramatically benefited from grain refinement, the microstructure refinement of magnesium alloys has become an important research field. Generally, there are two different approaches to grain refinement during solidification processing, which include chemical stimulation [4−6] and physical induction [7−9]. As the chemical route heavily relies on the selection of a nucleating catalyst, it is not always possible to find or develop a potent nucleus for a given group of alloys, for example, Mg−Al alloys [10−11]. This makes the physical method a favorable option for many cast alloys.

Nowadays, it has been proved that ultrasonic treatment is a simple and effective physical means for solidification control and grain refinement [12−13]. During the process of ultrasonic treatment, the extremely high temperature and pressure produced by collapses of cavitation bubbles play a critical part in grain refinement. Therefore, it is instructive and meaningful to study the behaviors of cavitation bubbles. However, due to the fact that cavitation bubbles are very tiny and their existing time is very short, it appears very difficult to directly observe ultrasonic cavitation in metal melt, which is a non-transparent fluid at high temperature. Thus, theoretical calculation turns to a feasible method to study the ultrasonic cavitation in metal melt [14−16]. On the other hand, many studies concerning ultrasonic treatment mainly focus on the as-cast grain refinement of low-melting alloys or aluminum alloys [17−18]. However, few works especially numerical simulations have been made on the application of ultrasonic vibration

Foundation item: Projects (2007CB613701, 2007CB613702) supported by the National Basic Research Program of China; Projects (50974037, 50904018) supported by the National Natural Science Foundation of China; Project (NCET-08-0098) supported by the Program for New Century Excellent Talents in University of China

Corresponding author: LE Qi-chi; Tel: +86-24-83683312; E-mail: lourry@163.com; qichil@mail.neu.edu.com

DOI: 10.1016/S1003-6326(11)61039-X

to the magnesium alloys. Therefore, in this work, ultrasonic field was introduced to AZ80 alloy melt to achieve the effect of grain refinement, and according to the basic theory of ultrasonic cavitation, the influences of different ultrasonic pressures on the behaviors of cavitation bubble in AZ80 alloy melt were investigated by virtue of numerical simulation solving Rayleigh-Plesset equation with Matlab. Besides, in order to gain a favorable cavitation effect in AZ80 alloy melt which in turn results in a good effect of grain refinement, it is necessary to get more information about ultrasonic field propagations in AZ80 alloy melt and thus numerical solution of the wave equation was carried out. Then, the influences of different global ultrasonic intensities on the spatial distribution of acoustic pressure and effects of grain refinement were both investigated.

2 Experimental apparatus and methods

As shown in Fig. 1, the experimental apparatus for ultrasonic treatment used in this study consisted of a resistance furnace, an iron crucible and a metallurgic ultrasonic system with power ranging from 0 to 2 kW, including an ultrasonic generator with frequency of (20±2) kHz, a magnetostrictive transducer and a mild steel made acoustic radiator (emitter area of 314 mm^2).

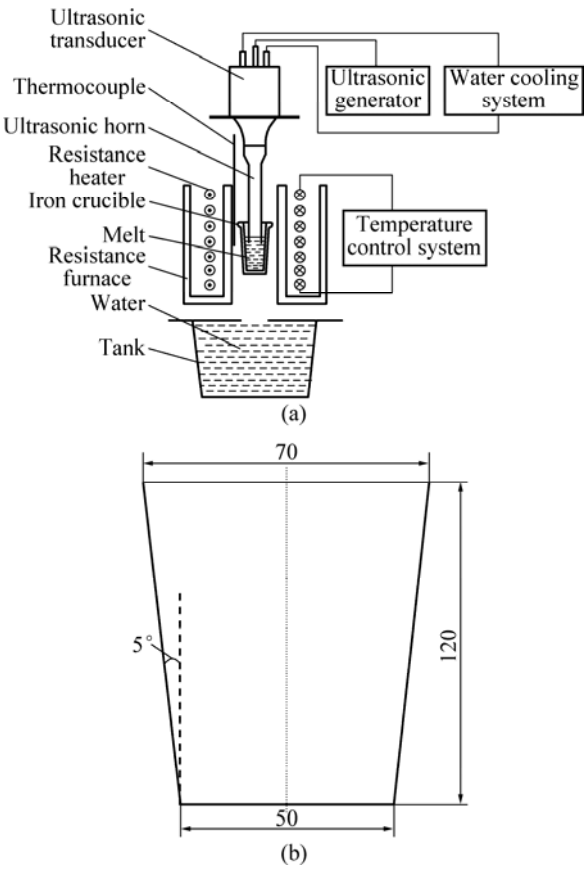

Fig. 1 Schematic diagram of experiment arrangement (a) and dimensions (b) of crucible used in experiment

One of the most typical magnesium alloys, AZ80 alloy was used in this investigation. During the treatment procedure, the temperature of the melt, the preheating temperature of the radiator and the time of applying the ultrasonic field were precisely controlled. Firstly, 550 g charge was melted in the iron crucible which was heated by a laboratory resistance furnace and protected by CO_2+0.5%SF_6 atmosphere. The melt was heated to 650 °C and controlled at this temperature for 600 s. The preheated ultrasonic horn at 650 °C was inserted 20 mm under the surface in the magnesium alloy melt and the height of the melt was nearly 120 mm. Then, the magnesium alloy melt was treated by ultrasonic vibration for 15 s and then it was immediately water quenched. For comparison, samples were also made without ultrasonic vibration.

After the cast alloy was cooled, the samples taken from different positions of cast were used for analyzing and testing. Two different methods were used to observe the microstructure of the ingot samples. Some samples were polished, etched with 4% nital and observed using Leica DMR Metalloscope; the other samples were polished, etched with a new corrosive agent, the chemical composition of which was 6.5 g picric acid, 100 mL ethyl alcohol, 10 mL distilled water and 5 mL glacial acetic acid, and observed under polarized light by Leica DMR Metalloscope. The grain size was evaluated by transversal method which calculated the average diameter of grain by counting the number of grains within 10 unit length in the 100 times enlarged field of view.

3 Numerical simulations

3.1 Numerical calculation of ultrasonic cavitation in magnesium alloy melt

It is believed that cavitation process is actually the motion process of cavitation bubble wall [19−20]. When a beam of ultrasound characterized as $P_m\sin\omega t$ propagates in the magnesium alloy melt, the tiny bubbles in the liquid are subjected to expansion and compression effects. Assume that both ultrasonic intensity and the bulk liquid temperature keep constant, the gas and vapor within cavitation bubbles and the liquid can be treated as incompressible ideal gas and incompressible continuum, respectively, the partial pressure of vapor within cavitation bubble equals its counterpart of bulk liquid, and the motion of cavitation bubble wall meets spherical symmetric movement. Considering the influences of liquid viscosity, surface tension and vapor pressure on the movement of bubble wall, the basic kinematic equation of bubble wall under the action of acoustic wave can be finally obtained based on the continuity equation and motion equation of bubbles, which is also

known as the famous Rayleigh-Plesset equation [21−22] as

$$\rho\left[R\left(\frac{\mathrm{d}^2R}{\mathrm{d}t^2}\right)+\frac{3}{2}\left(\frac{\mathrm{d}R}{\mathrm{d}t}\right)^2\right]=\left(P_0+\frac{2\sigma}{R_0}\right)\left(\frac{R_0}{R}\right)^{3K}-\frac{2\sigma}{R}-\frac{4\eta}{R}\left(\frac{\mathrm{d}R}{\mathrm{d}t}\right)-P_0+P_\mathrm{v}+P_\mathrm{m}\sin\omega t \quad (1)$$

where R and R_0 are the instantaneous radius and initial radius of bubble, respectively; P_0, P_v and P_m are the initial pressure outside cavitation bubble, vapor pressure within cavitation bubble and acoustic pressure amplitude, respectively; σ is the surface tension; η is the fluid viscosity; K is the polytropic exponent and ω is the angular frequency of the acoustic wave, given by $\omega=2\pi f$.

3.2 Field modelling of ultrasonic propagation in magnesium alloy melt

In order to study the ultrasonic field propagation, numerical simulations are carried out. As linear wave propagation is assumed and the shear stress is neglected, the acoustic pressure P can be obtained by solving the wave equation as

$$\nabla\left(\frac{1}{\rho}\nabla P\right)-\frac{1}{\rho c^2}\frac{\partial^2P}{\partial t^2}=0 \quad (2)$$

where ρ is the density of the melt; c is the speed of the sound in the melt and t is time. With the time harmonic assumption, a solution of the form is obtained as

$$P(r,z,t)=p(r,z)\mathrm{e}^{i\omega t} \quad (3)$$

where ω is the angular frequency and the spatial variation of the acoustic pressure $p(r, z)$ can be given by the solution of the homogeneous Helmholtz equation as

$$\nabla\left(\frac{1}{\rho}\nabla p\right)+\frac{\omega^2}{\rho c^2}p=0 \quad (4)$$

The intensity distribution $I(r, z)$ can be obtained as

$$I(r,z)=\frac{p^2(r,z)}{2\rho c} \quad (5)$$

The homogenous Helmholtz equation is solved by the finite element method. It should be noted that in order to obtain an accurate numerical solution of the Helmholtz equation, the discretization stepsize h should be adjusted to satisfy the following equation [23−25]:

$$kh=A \quad (6)$$

where k is the wave number ($k=\omega/c$) and A is a constant. However, under this condition, the errors of the finite element solution grow sharply as the wave number k increases, which is termed as pollution effect [26−27]. To overcome this problem, an adequate refined mesh is used [28−29]. Finally, the following boundary conditions are obtained:

1) $p=0$ at the liquid-air interfaces corresponding to a total reflection condition as soft walls;

2) $p=p_0$ at the horn tip, where p_0 is the amplitude of the wave;

3) $\partial p/\partial n=0$ at the side walls of the horn which represents hard walls;

4) $1/\rho(\partial p/\partial n)+i\omega p/Z=0$ at the walls of the crucible which represents the impedance boundary condition and here Z is the acoustic input impedance of the external domain.

4 Results and discussion

4.1 Numerical calculation of ultrasonic cavitation in melt

When the numerical calculation of ultrasonic cavitation is carried out, it is assumed that the density of the melt ρ is 1 700 kg/m^3, the surface tension σ is 0.564 N/m, the initial pressure outside cavitation bubble P_0 is 1.013×10^5 Pa, the vapor pressure within cavitation bubble P_v is 1 000 Pa, the fluid viscosity η is 1.12×10^{-3} Pa·s and the polytropic exponent K is 1.33.

4.1.1 Selection of frequency of ultrasonic wave

In this work, research on the effect of global ultrasonic intensities on the gain refinement is carried out. However, the frequency of ultrasonic wave should be chosen first and therefore Rayleigh-Plesset equation with different frequencies is solved. The initial radius of bubble R_0 is assumed as 4.5 μm and the applied ultrasonic pressure is 1 MPa. Figure 2 presents the behavior of bubbles in the magnesium alloy melt which is treated by ultrasonic field with different frequencies. When the ultrasonic frequency is 20 kHz, the bubble expends to 98 times of its initial size and then collapses within 54 μs. As ultrasonic frequency increases to 25, 30 and even 50 kHz, the bubble expands to 78, 65 and 39 times of its initial size and then collapses within 43, 36 and 22 μs, respectively. When the frequency continues to increase to 100 kHz, the bubble does not collapse after first expansion, but it shrinks and then expands to 43 times of its initial size before its final collapse within 52 μs. After the ultrasonic frequency increases to 300 kHz, the bubble pulsates and expands to the maximum 31 times of its initial size, but it does not collapse within 120 μs. The results show that the trembling strength of cavitation bubble indicated by the maximum ratio of R to R_0 is the largest when the ultrasonic frequency is 20 kHz, and basically with the increase of ultrasonic frequency, the trembling strength becomes weaker. Therefore, ultrasonic wave with the frequency of 20 kHz has the most effective cavitation. In this work, ultrasonic wave

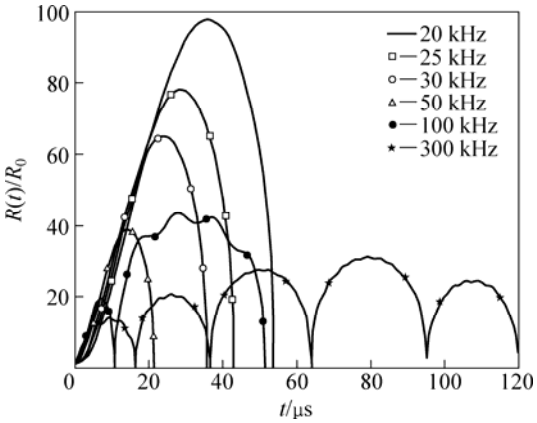

Fig. 2 Behavior of bubble in molted magnesium during treatment by ultrasonic field with different frequencies (R_0 is 4.5 μm and applied ultrasonic pressure is 1 MPa)

with the frequency of (20±2) kHz is selected.

4.1.2 Influence of acoustic pressure on ultrasonic cavitation

After the ultrasonic frequency is chosen, the influence of acoustic pressure on ultrasonic cavitation is studied. The initial radius of bubble R_0 is assumed to be 4.5 μm and the applied ultrasonic pressure frequency is 20 kHz. As shown in Fig. 3(a), when the acoustic pressure amplitude is 0.1 or 0.2 MPa, the bubble in metal melt continuously slightly oscillates nonlinearly, as a series of sinusoidal movement. After the acoustic pressure amplitude increases higher than 0.25 MPa, bubble trembles several periods and its life only lasts for less than 120 μs (see Fig. 3(b)). It can also be seen that with the elevation of acoustic pressure amplitude, the trembling strength is accordingly intensified, which means that a higher acoustic pressure makes a more effective ultrasonic cavitation.

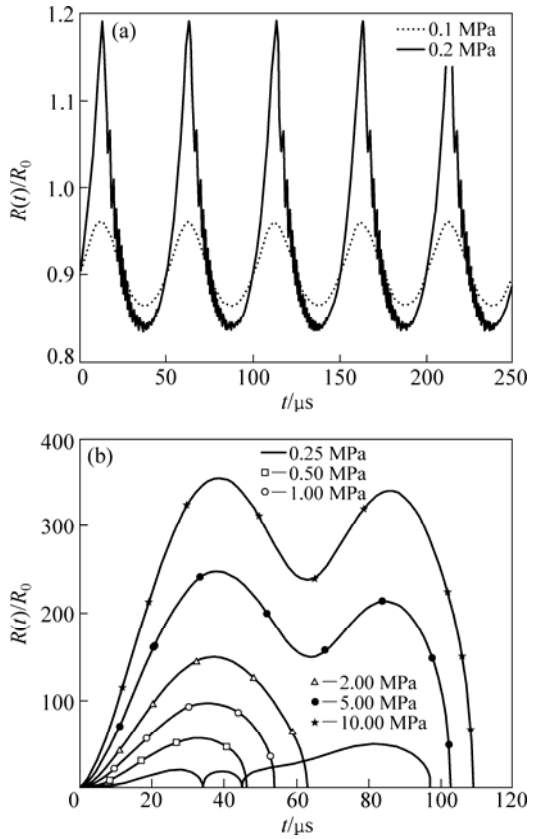

Fig. 3 Behavior of bubble in molted magnesium during treated by ultrasonic field with different acoustic pressures (R_0 is 4.5 μm and applied ultrasonic frequency is 20 kHz): (a) P_m= 0.1 and 0.2 MPa; (b) P_m=0.25−10 MPa

4.2 Acoustic field modelling and relevant experiment

According to the fact that the velocity of ultrasound in magnesium alloy melt at 650 °C is almost 4 000 m/s [30−31], a wavelength of 200 mm is chosen for modeling which corresponds to the propagation of 20 kHz ultrasound in magnesium melt and the acoustic input impedance of the iron crucible is assumed to be 4.2×10^7 Pa·s/m. Figure 4 presents the calculated spatial variation of the acoustic pressure $p(r, z)$ in magnesium alloy melt for global ultrasonic intensity of 30.48 W/cm^2. It can be seen that it is in agreement with Ref. [32], within certain geometry of the crucible, relatively high values of pressure (including both positive and negative) which assist the cavitation events are not only found in close vicinity of the horn tip but also other areas. It is totally different from the traditional assumption that as the distance from the horn tip increases, the pressure decreases accordingly to an increasing area into which it is spread.

The final use of this information concerning ultrasonic field propagations in magnesium alloy melt is to obtain a favorable cavitation effect which in turn results in a good effect of grain refinement in ingot [33−34], and relevant experiments are carried out. As shown in Fig. 4, the samples taken from different positions *A*, *B* and *C*, which correspond to the distance from emitter of 25, 50 and 75 mm, respectively, are used for analyzing and testing. The microstructure of as-cast AZ80 alloy from these three positions after ultrasonic

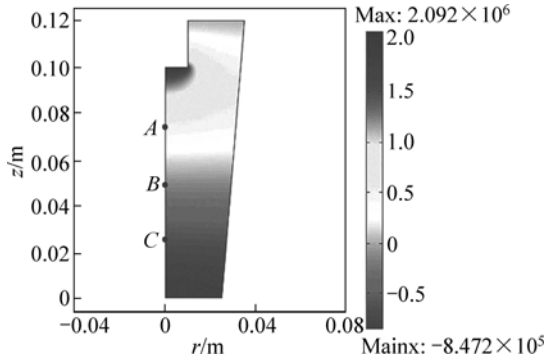

Fig. 4 Pressure field $p(r, z)$ for global ultrasonic intensity of 30.48 W/cm^2

treatment with global ultrasonic intensity of 30.48 W/cm^2 for 15 s and typical microstructure of samples without ultrasonic treatment are compared and discussed. It is found that without ultrasonic treatment, the microstructure is characterized with developed dendrite structure and the average grain size of the sample is about 302 μm; however, after ultrasonic treatment, with the increase of distance from emitter, grains of AZ80 alloy initially become more coarse from positions *A* to *B*, but when it comes to position *C*, the grain is refined again, as shown in Fig. 5. It indicates that different positions make different effect of gain refinement and the average grain sizes of samples from positions *A*, *B* and *C* are 169, 263 and 197 μm, respectively. On the other hand, the results of numerical simulation (see Fig. 4) indicate that positions *A*, *B* and *C* are subjected to about 0.53, −0.11 and −0.65 MPa acoustic pressure, respectively. Hence, according to the results of numerical simulation of ultrasonic cavitation, a higher acoustic pressure makes a more intensive ultrasonic cavitation. It is easy to understand that the sample from position *B* with the least acoustic pressure has the poorest effect of grain refinement. However, it seems controversial that the sample from position *C* with a maximum acoustic pressure of the three which is supposed to experience the most intensive ultrasonic cavitation is not the one with the finest grain. In fact, cavitation which took place at high acoustic pressure is a highly energy-consuming process and consequently the absorption coefficient can be considerably high [32, 35]. Unfortunately, the wave equation in the paper obviates the absorption contribution. Thus, the acoustic pressure of position *C* is magnified to a certain degree mainly because of the omission of absorption of ultrasound in magnesium alloy melt, which will be modified in further work.

The influences of different global ultrasonic intensities on the spatial distribution of acoustic pressure and effect of grain refinement are both investigated. Figure 6 shows the variation of pressure in the centre of the transducer along the axial direction for different ultrasonic intensity of 2.44, 9.65, 20.32, 30.48 and 47.41 W/cm^2, respectively. It can be found that with the increase of global ultrasonic intensity, the acoustic pressure in corresponding position is also enlarged except for where the pressure is 0. Figure 7 presents the effect of global ultrasonic intensity on the grain size of AZ80 alloy after 20 kHz ultrasonic treatment for 15 s and all these samples are taken from the position which is 20 mm from the emitter in the axial direction. Basically, with the augmentation of global ultrasonic intensity, the average grain size of samples accordingly decreases. The results indicate that a greater global ultrasonic intensity leads to a strong increase in acoustic pressure and therefore a better effect of grain refinement.

The microstructures of as-cast AZ80 alloy observed under polarized light with and without ultrasonic treatment are shown in Fig. 8. Without subject to ultrasonic vibration, the dendrites were coarse and large,

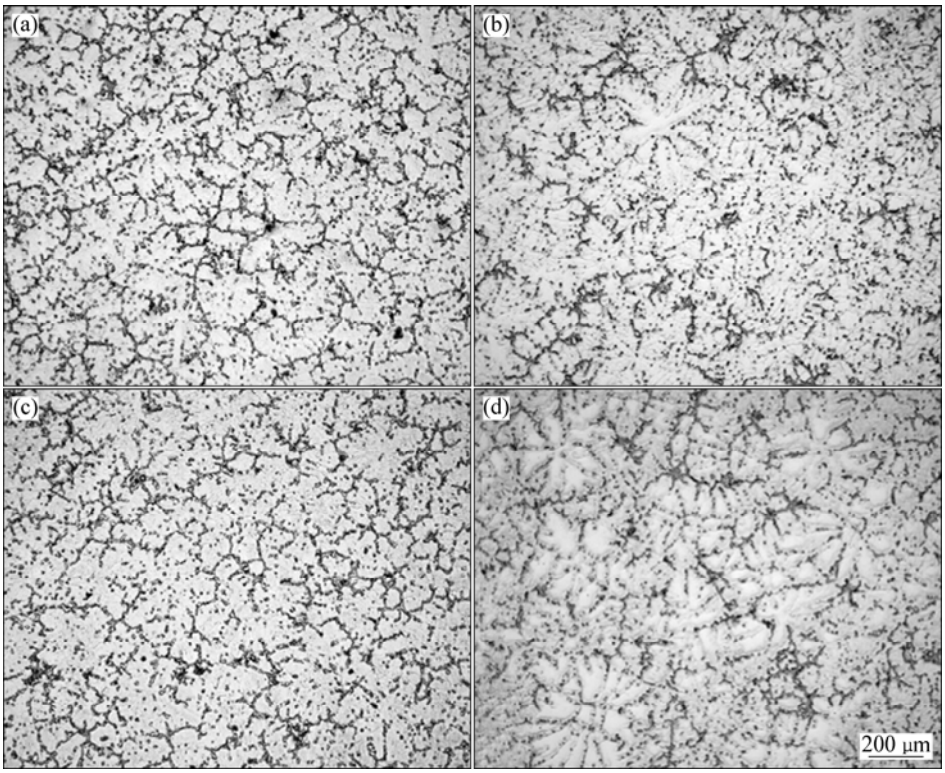

Fig. 5 SEM images of ingot samples of AZ80 alloy with (a−c) and without (d) ultrasonic treatment from different positions in Fig. 4: (a) *A*; (b) *B*; (c) *C*; (d) Without ultrasonic treatment

and the average grain size is about 303 μm. After ultrasonic treatment, globular grains are obtained in the AZ80 alloy and the minimum of the average grain size is 148 μm when the ultrasonic intensity is 30.48 W/cm^2. Generally, with the increase of ultrasonic intensity, the grains are continued to be refined. Thus, in order to

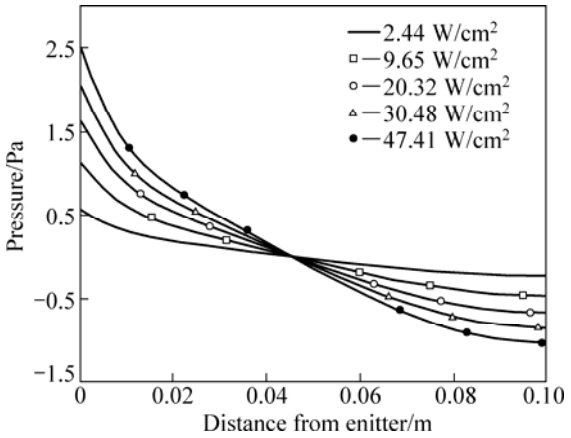

Fig. 6 Pressure profile in center of transducer along axial direction for different global ultrasonic intensities

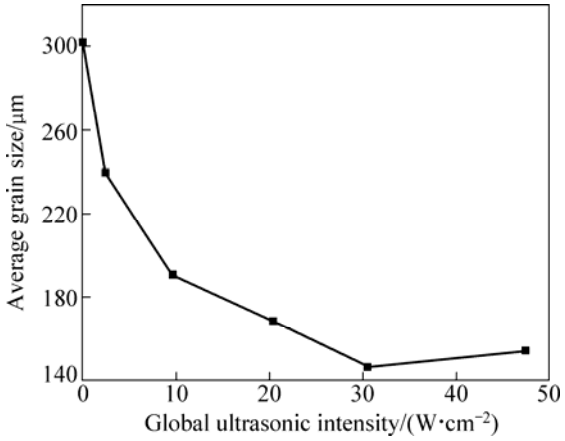

Fig. 7 Effect of global ultrasonic intensity on grain size of AZ80 alloy after 20 kHz ultrasonic treatment for 15 s

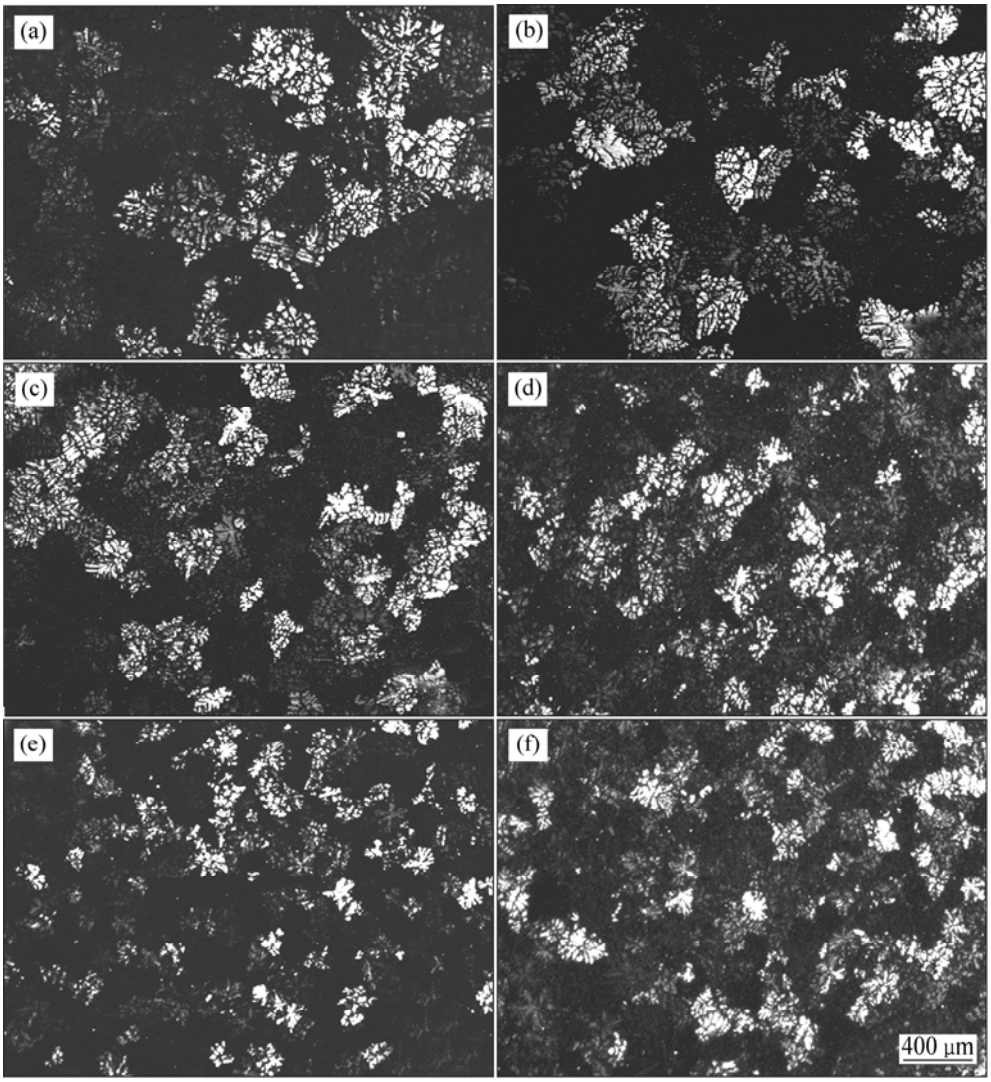

Fig. 8 SEM images under polarized light in ingot samples of AZ80 alloy without ultrasonic treatment (a), with ultrasonic treatment at global ultrasonic intensities of 2.44 W/cm^2 (b), 9.65 W/cm^2 (c), 20.32 W/cm^2 (d), 30.48 W/cm^2 (e) and 47.41 W/cm^2 (f)

obtain a favorable effect of grain refinement by virtue of ultrasonic treatment, a strong enough global ultrasonic intensity is needed.

5 Conclusions

1) With a higher acoustic pressure exceeding the cavitation threshold, more intensive effect of ultrasonic cavitation is obtained.

2) Different positions of the sample, which are subjected to different acoustic pressures during ultrasonic treatment for its AZ80 alloy melt, have different effect on the gain refinement.

3) A stronger global ultrasonic intensity leads to a strong increase in acoustic pressure and therefore a better effect of grain refinement.

References

[1] MORDIKE B L, EBERT T. Magnesium: Properties applications potential [J]. Materials Science and Engineering A, 2001, 302(1): 37−45.

[2] LETZIG D, SWIOSTEK J, BOHLEN J, BEAVEN P A, KAINER K U. Wrought magnesium alloys for structural applications [J]. Material Science and Technology, 2008, 24(8): 991−996.

[3] PAN Fu-sheng, HAN En-hou. High-performance magnesium alloys and their processing technologies [M]. Beijing: Science Press, 2007: 59−70. (in Chinese).

[4] NOGITA K, DAHLE A K. Effects of boron on eutectic modification of hypoeutectic Al-Si alloy [J]. Scripta Materialia, 2003, 48(3): 307−313.

[5] LU L M, DAHLE A K, St JOHN D H. Grain refinement efficiency and mechanism of aluminium carbide in Mg−Al alloys [J]. Scripta Materialia, 2005, 53(5): 517−522.

[6] EMLEY E F. Principles of magnesium technology [M]. Oxford: Pergamon Press, 1966: 47−65.

[7] GUO Shi-jie, LE Qi-chi, ZHAO Zhi-hao, CUI Jian-zhong. Microstructural refinement of DC cast AZ80 Mg billets by low frequency electromagnetic vibration [J]. Materials Science and Engineering A, 2005, 404(1): 323−329.

[8] ESKIN G I. Broad prospects for commercial application of the ultrasonic (cavitation) melt treatment of light alloy [J]. Ultrasonics Sonochemistry, 2001, 8(3): 319−325.

[9] RAMIREZ A, MA Q, DAVIS B, WILKS T, St JOHN D H. Potency of high-intensity ultrasonic treatment for grain refinement of magnesium alloys [J]. Scripta Materialia, 2008, 59(1): 19−22.

[10] St JOHN D H, MA Q, EASTON M A. Grain refinement of magnesium alloys [J]. Metall Mater Trans A, 2005, 36(7): 1669−1679.

[11] LEE Y C, DAHLE A K, STJOHN D H. The role of solute in grain refinement of magnesium [J]. Metall Mater Trans A, 2000, 31(11): 2895−2906.

[12] GAO De-ming, LI Zhi-jun, HAN Qing-you, ZHAI Qi-jie. Effect of ultrasonic power on microstructure and mechanical properties of AZ91 alloy [J]. Materials Science and Engineering A, 2009, 502(1): 2−5.

[13] LI Xin-tao, LI Ting-ju, LI Xi-meng, JIN Jun-ze. Study of ultrasonic melt treatment on the quality of horizontal continuously cast Al−1%Si alloy [J]. Ultrasonics Sonochemistry, 2006, 13(2): 121−125.

[14] ESKIN G I. Ultrasonic treatment of light alloy melts [M]. Amsterdam: Gordon & Breach, 1998: 14−28.

[15] FRANC J P. The Rayleigh-Plesset equation: A simple and powerful tool to understand various aspects of cavitation [J]. CISM Courses and Lectures, 2007, 491(1): 1−41.

[16] LIU Rong-guang, LI Xiao-qian, HU Shi-cheng. Process simulation of ultrasonic generated cavitation effect in aluminum alloy fusant and the process evolution of air bubble [J]. China Foundry Machinery & Technology, 2007, 6(3): 16−19. (in Chinese)

[17] JIAN X G, THOMAS T M, HAN Q Y. Refinement of eutectic silicon phase of aluminum A356 alloy using high-intensity ultrasonic vibration [J]. Scripta Materialia, 2006, 54(5): 893−896.

[18] ABRAMOV V, ABRAMOV O, BULGAKOV V, SOMMER F. Solidification of aluminium alloys under ultrasonic irradiation using water-cooled resonator [J]. Materials Letters, 1998, 37(1): 27−34.

[19] MA Li-qun, LIAO Heng-cheng. Numerical research on movement of cavitation bubble in metal melt under high intensity ultrasound [J]. Journal of Southeast University, 1998, 28(4): 145−149. (in Chinese)

[20] NOLTINGK B E, NEPPIRAS E A. Cavitation produces by ultrasonics [J]. Proc Phys Soc, 1950, 63(9): 674−685.

[21] PROSPERETTI A. Physics of acoustic cavitation [J]. Frontiers in Physical Acoustics, 1986(1): 145−183.

[22] JAMES R, MUTHUPANDIAN A, OLIVIER E, CLEMENS V S, JACQUES R, FRANZ G. Estimation of ultrasound induced cavitation bubble temperatures in aqueous [J]. Ultrasonics Sonochemistry, 2005, 12(5): 325−329.

[23] IHLENBURG F, BABUŠKA I. Finite element solution to the Helmholtz equation with high wave number. Part I: The h-version of the FEM [J]. Comput Math Appl, 1995, 30(9): 9−37.

[24] HARARI I, HUGHES T J R. Finite element methods for the Helmholtz equation in an exterior domain: model problems [J]. Comput Methods Appl Mech Engrg, 1991, 87(1): 59−96.

[25] BABUŠKA I, IHLENBURG F, STROUBOULIS T, GANGARAJ S K. A posterior error estimation for finite element solutions of Helmholtz equation. Part I: The quality of local indicators and estimators [J]. Int J Numer Meth Eng, 1997, 40(1): 3443−3462.

[26] BABUŠKA I, IHLENBURG F, PAIK E T, SAUTER S A. A generalized finite element method for solving the Helmholtz equation in two dimensions with minimal pollution [J]. Comput Math Appl, 1995, 128(4): 325−359.

[27] IHLENBURG F, BABUŠKA I. Dispersion analysis and error estimation of Galerkin finite element methods for the Helmholtz equation [J]. Int J Numer Meth Eng, 1995, 38(22): 3745−3774.

[28] SÁEZ V, FRÍAS-FERRER A, INIESTA J, GONZÁLEZ-GARCÍA J, ALDAZ A, RIERA E. Chacterization of a 20kHz sonoreactor. Part I: Analysis of mechanical effects by classical and numerical methods [J]. Ultrasonics Sonochemistry, 2005, 12(1): 59−65.

[29] LOUISNARD O, GONZALEZ-GARCIA J, TUDELA I, KLIMA, J, SAEZ V, VARGAS-HERNANDEZ Y. FEM simulation of a sono-reactor accounting for vibrations of the boundaries [J]. Ultrasonics Sonochemistry, 2009, 16(2): 250−259.

[30] BLAIRS S. Correlation between surface tension, density, and sound velocity of liquid metals [J]. Journal of Colloid and Interface Science, 2006, 302(1): 312−314.

[31] MCALISTER S P, CROZIER E D, COCHRAN J F. Compressibility and concentration fluctuations in liquid magnesium alloys [J]. J Phys C: Solid State Phys, 1973, 6(14): 2269−2278.

[32] KLÍMA J, FRÍAS-FERRER A, GONZÁLEZ-GARCÍA J, LUDVÍK J, SÁEZ V, INIESTA J. Optimisation of 20kHz sonoreactor geometry on the basis of numerical simulation of local ultrasonic intensity and

qualitative comparison with experimental results [J]. Ultrasonics Sonochemistry, 2007, 14(1): 19−28.

[33] MA Q, RAMIREZ A, DAS A. Ultrasonic refinement of magnesium by cavitation: clarifying the role of wall crystals [J]. J Cryst Growth, 2009, 311(14): 3708−3715.

[34] LIU X B, OSAWA Y, TAKAMORI S, MUKAI T. Grain refinement of AZ91 alloy by introducing ultrasonic vibration during solidification [J]. Materials Letters, 2008, 62(17): 2872−2875.

[35] MA Q, RAMIREZ A. An approach to assessing ultrasonic attenuation in molten magnesium alloys [J]. J Appl Phys, 2009, 105: 01358.

超声细化处理 AZ80 镁合金过程中的声场数值模拟

邵志文，乐启炽，张志强，崔建忠

东北大学 材料电磁过程教育部重点实验室，沈阳 110004

摘　要：采用不同强度超声对 AZ80 镁合金熔体进行处理以改善合金的凝固组织。当施加的超声强度为 30.48 W/cm^2 时，合金的平均晶粒尺寸由未经超声处理时的 303 μm 降低为 148 μm。为了进一步了解超声改善镁合金微观组织的机理，采用数值模拟的方法研究超声声压对空化泡行为的影响，并且对熔体中的超声场分布情况进行分析。结果表明，熔体内不同位置所受的声压是不同的，因此不同位置上的铸锭试样的晶粒细化程度也不同。随着超声强度的增加，声压值增加，而合金的晶粒尺寸则随之降低。

关键词：数值模拟；声压；超声处理；晶粒细化；镁合金

(Edited by FANG Jing-hua)